

EFDA–JET–CP(07)03/27

R.V. Budny, E. Mazzucato, J. Candy, R.E. Waltz, R. Bravenec, A. Fonseca,  
the TFTR team and JET EFDA contributors

# Gyrokinetic Simulations of Electron Density Fluctuations and Comparisons with Measurements

"This document is intended for publication in the open literature. It is made available on the understanding that it may not be further circulated and extracts or references may not be published prior to publication of the original when applicable, or without the consent of the Publications Officer, EFDA, Culham Science Centre, Abingdon, Oxon, OX14 3DB, UK."

"Enquiries about Copyright and reproduction should be addressed to the Publications Officer, EFDA, Culham Science Centre, Abingdon, Oxon, OX14 3DB, UK."

# Gyrokinetic Simulations of Electron Density Fluctuations and Comparisons with Measurements

R.V. Budny<sup>1</sup>, E. Mazzucato<sup>1</sup>, J. Candy<sup>2</sup>, R.E. Waltz<sup>2</sup>, R. Bravenec<sup>3</sup>, A. Fonseca<sup>4</sup>,  
the TFTR team and JET EFDA contributors\*

<sup>1</sup>*PPPL, Princeton NJ, USA*

<sup>2</sup>*GA, San Diego CA, USA*

<sup>3</sup>*Univ. Texas, Austin, TX, USA*

<sup>4</sup>*CFN-IST, IT, Port*

*\* See annex of M.L. Watkins et al, "Overview of JET Results ",  
(Proc. 21<sup>st</sup> IAEA Fusion Energy Conference, Chengdu, China (2006)).*

Preprint of Paper to be submitted for publication in Proceedings of the  
34th EPS Conference on Plasma Physics,  
(Warsaw, Poland 2nd - 6th July 2007)



## INTRODUCTION

Understanding transport is important for creating reliable predictions of plasma performance in fusion reactors. Plasma turbulence causes much of the transport seen in present experiments. Gyrokinetic codes can simulate turbulence and turbulent-driven transport. Further verifying and validating these simulations are needed. One class of tests is provided by electron density fluctuation  $\tilde{n}_e$  measurements using techniques such as reflectometry and beam-emissionspectroscopy.

The GYRO gyrokinetic code [1] is being used to simulate turbulence and turbulent-driven energy, angular momentum, and species flows in experiments. GYRO can generate the timeevolving fluctuations of  $\tilde{n}_e$  in three spatial dimensions. From this, profiles, along the diagnostic lines-of-sight, of the root-mean-square  $\tilde{n}_e$ , radial correlation lengths  $\lambda_r$ , and power spectra can be produced. This paper focuses on GYRO simulations of reflectometry measurements in TFTR and JET. These are the first published nonlinear gyrokinetic fluctuation simulations for either tokamak.

## FLUCTUATION MEASUREMENTS

On TFTR and JET, fluctuations measurements were performed using tunable microwave reflectometers operating in the X-mode ( $\vec{E} \perp \vec{B}_{TF}$ ) in the ranges of frequencies 132-140GHz (TFTR) and 92-96 and 100-106GHz (JET). Radial correlation measurements were performed at several plasma radial locations by stepping the relative frequency in pairs of reflectometers every 20 msec over a range of  $\approx 3$ GHz.

In the presence of large levels of plasma turbulence, as described in Ref. [2], the radial correlation of measured signals becomes smaller than that of plasma fluctuations. The TFTR measurements were corrected using the random phase screen model [2] where the primary effect of density fluctuations is to modulate the phase of the probing wave near the cutoff by an amount given by the geometric optics approximation, and by assuming for the latter a Gaussian distribution. In the case of JET no attempt has been made yet for correcting the measured signal correlations.

## SIMULATIONS

The GYRO simulations are based on measured plasma profiles and the magnetic flux geometry. The densities of three kinetic species - electron and two ion species (bulk and one effective impurity maintaining charge neutrality) - were derived using the TRANSP plasma analysis code [3] The radial simulation domain extends over about half the minor radius. Up-down symmetrized Miller equilibria, trapping, and electron-ion collisions are included. The ranges of wavenumbers include the ITG and TEM modes ( $k_\theta \rho_s$  up to  $\approx 1.0$  with  $k_\theta$  the perpendicular wavenumber and  $\rho_s$  the ion sound speed gyro-radius). The saturated nonlinear turbulence is calculated using the electrostatic approximation, which is expected to be accurate for the plasmas considered. The mean-value flow-shearing rates play important roles in suppressing the turbulence in saturation. We calculate these from  $E_r$  which is calculated from force balance using the measured carbon  $v_{tor}$ , pressure, and neoclassical  $v_{pol}$ . Also the simulated zonal flows play an important role in saturating the turbulence.

## DATA ANALYSIS

The electron density is calculated from the first moment of the perturbed electron distribution function. Coefficients that are functions of  $r$ ,  $n$  (the toroidal mode number),  $t$ , and from which the rapid variation with poloidal angle  $\theta$  and toroidal angle  $\phi$  have been extracted are written to a GYRO output file at chosen values of  $\theta$ . These are read by a utility code which linearly interpolates them onto a fine  $\theta$  grid and multiplies by  $\exp\{-in[\nu(r, \theta) - \omega_{eb0}t]\}$  to restore the rapid  $\theta$  variation. (We take  $\phi = 0$ .) Here  $\nu(r, \theta)$  is the rigorous representation of  $q(r)$  and  $\omega_{eb0}$  is the equilibrium  $E \times B$  frequency at the center of the simulation domain (on the outer midplane) to account for an overall Doppler shift. Finally, the code sums over  $n$  and takes the real part to obtain  $n_e(r, \theta, t)$ . From this we can construct  $\tilde{n}_e$  along the sight lines.

## RESULTS

We compare results with measurements in TFTR and JET. The JET plasmas are from a *BTF* scan in L-mode for studying fundamental D ICRH. They had  $I_p = 2.0\text{MA}$ ,  $B_{TF} = 3.4$  or  $3.8\text{T}$ ,  $6\text{MW}$  of D neutral beam injection,  $1.8\text{MW}$  ICRH, and low  $\beta_n (= 0.45)$  and Greenwald fraction ( $= 0.3$ ). GYRO simulations of energy and angular momentum transport are in approximate agreement with TRANSP. Figure 1 shows profiles of  $\tilde{n}_e / \langle n_e \rangle$  and the root-mean-square variance of  $\tilde{n}_e / \langle n_e \rangle$  (where  $\langle \tilde{n}_e / \langle n_e \rangle \rangle$  denotes local time averaging). These typically increase from very low values ( $< 10^{-4}$ ) within  $r/a$  of  $0.3$  to a up to a few percent at  $r/a$  around  $0.7$ . Figure 2 shows profiles of the  $\tilde{n}_e$  radial correlation function at several radii and the correlation length  $l_r$ . The radii with measurements are in approximate agreement with the simulations. The power spectra of the density is also simulated. Examples are shown in Figure 3. These do not agree well with the measurements, and the reasons for disagreement are not understood.

The TFTR measurements [4] were in a well-matched pair of supershots, one with D plasma and the other with DT. They have  $16\text{ MW}$  of neutral beam injection (D-only in one, and T-only in the other),  $I_p = 1.6\text{MA}$ ,  $B_{TF} = 4.7\text{T}$ , and  $\beta_n = 1.7$ . Both the measured and simulated root-mean-square  $\tilde{n}_e$  fluctuations and  $\lambda_r$  at two radii were nearly the same in both plasmas, and agree with each other to within roughly a factor of two. Results are shown in Fig.4.

## DISCUSSION

It is paradoxical that the TFTR pair have similar levels of  $\tilde{n}_e$  since they exhibit the strong effect of isotopic mass in the ion energy confinement generally observed in supershots (for instance  $T_i$  in the core of the DT plasma is about 30% higher than in D, and  $\chi_i^{tot}$  from TRANSP analysis is about one-third that in D). The effect is much stronger than the gyro-Bohm dependence ( $M^{-0.5}$ ) implied by naive gyrokinetic simulations of ITG/TEM turbulence if the turbulence drive and damping were the same.

The GYRO simulations of energy and angular momentum transport in the D and DT supershots using measured profiles and nominal  $E_r$  are higher than the values inferred from TRANSP analysis.

The simulated  $\chi_i^D$  is about twice the TRANSP  $\chi_i^{DT}$  and  $\chi_e^{DT}$  is about twice  $\chi_e^D$ . These results depend sensitively on assumed input profiles such as the gradients of temperatures, densities, and flow-shearing rate. For instance, a 20% reduction of  $|\nabla(T_i)|$  would bring the simulations considerably closer to the TRANSP-analysis values. Since  $E_r$  was not measured directly, we also performed simulations with the flow-shearing rate increased by 20% for comparison. One noteworthy difference in the pair is that the computed  $E_r$  is higher in the DT plasma by a factor of two. This difference appears to be significant in reducing the transport.

The energy and angular momentum transport in the JET L-mode pair are also not simulated as accurately as  $\tilde{n}_e$ . Thus it appears harder for GYRO to accurately simulate transport than  $\tilde{n}_e$  in general, perhaps due to increased sensitivity to profiles or to the need to simulate several variables and their relative phases accurately.

## ACKNOWLEDGEMENTS

We wish to thank the US Department of Energy for supporting this research under Contract No. DE-ACO2-CHO3073

## REFERENCES

- [1]. J.Candy and R.E. Waltz, Phys. Rev. Lett., **91** (2003) 045001.
- [2]. E. Mazzucato and R. Nazikian, Phys. Rev. Lett. **12** (1993) 1840.
- [3]. R.V. Budny, D.R. Ernst, T.S. Hahm, D.C. McCune, *et al.*, Phys. Plasmas **7** 5038 (2002).
- [4]. E. Mazzucato, R.Nazikian, and S.Scott, 22th EPS, Bournemouth, 1995 Vol IV, p109.

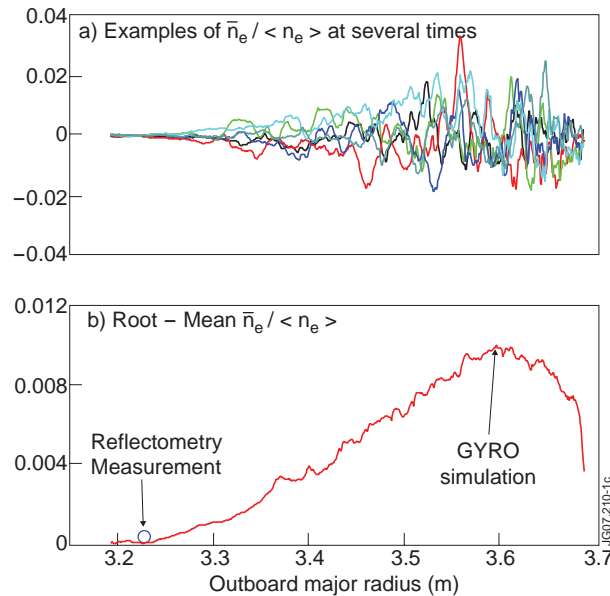


Figure 1: GYRO simulation and reflectometry measurement of  $n_e$  fluctuations in a JET L-mode plasma. The magnetic axes and out-board separatrices are at 2.97 and 3.85 m. a) profiles of  $\bar{n}_e/n_e$  at several times, b) profile of root-mean-square of the GYRO simulation. Both the simulation and the measurement are below about 0.02% at the one radius where the measurement could be made. Error bars are not yet available.

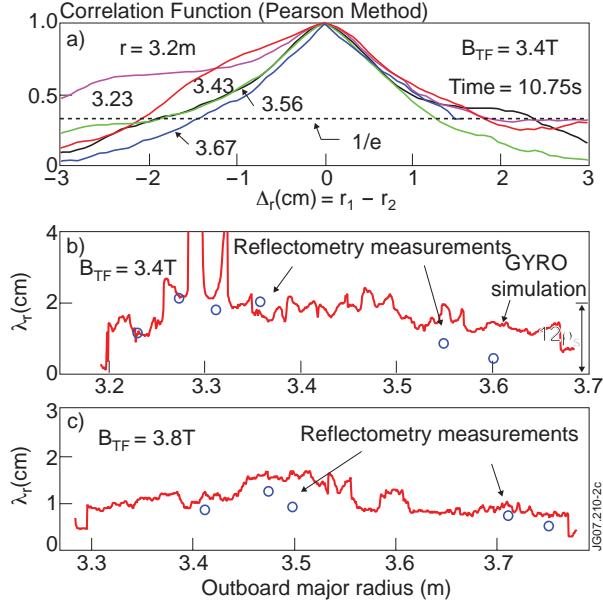


Figure 2: Simulation and measurements of radial  $\tilde{n}_e$  correlations in a pair of JET L-mode shots; a) Examples of the correlation function which is computed at each radius, and from which the average of the distances to larger and smaller radii where the correlation first drops below  $1/e$  is used to define the correlation length  $\lambda_r$ ; b)  $\lambda_r$  for the shot with  $B_{TF}=3.4T$ ; c)  $\lambda_r$  for the other shot with  $B_{TF}=3.8T$  (at the magnetic axis).

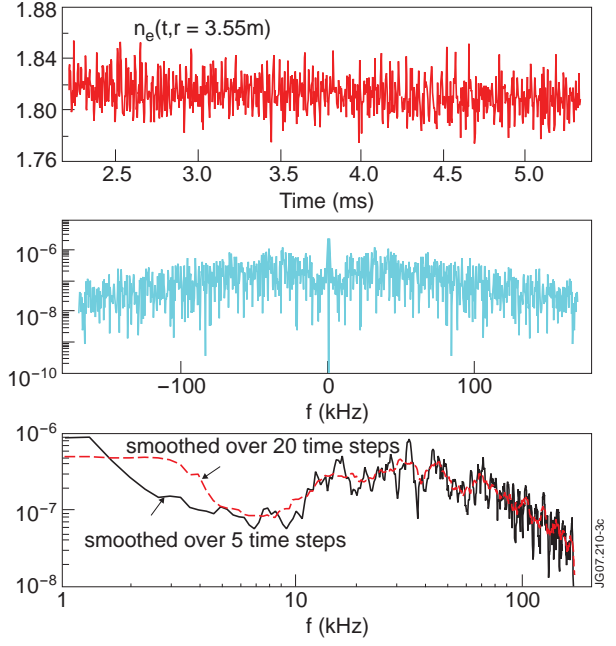


Figure 3: Simulation of  $\tilde{n}_e$  power spectra in a JET L-mode plasma. a) an example of the simulated  $\tilde{n}_e(t)$  at the location (in 3D) of one of the measurements; b) fast Fourier transform versus frequency; c) time-smoothed re-plotting of b).

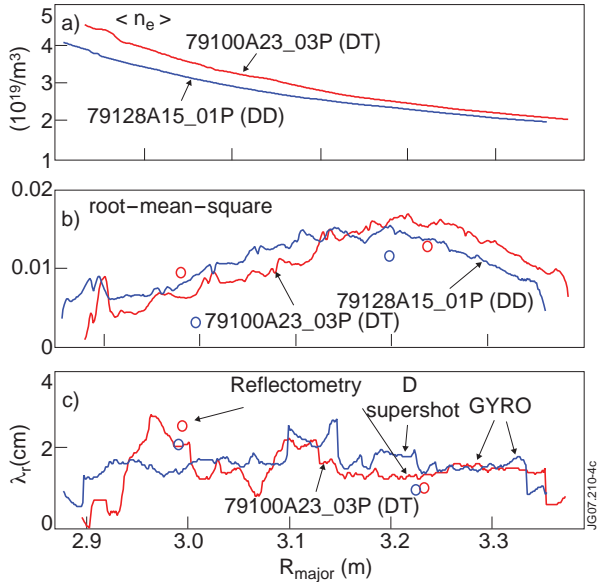


Figure 4: GYRO simulations of  $\tilde{n}_e$  and measurements in a matched pair of TFTR supershots; profiles. The magnetic axes and our-board last-closed magnetic surfaces are at 2.77 and 3.40m. a) reconstructed  $\langle n_e \rangle$ , b) root-mean-square  $\tilde{n}_e / \langle n_e \rangle$ , and c)  $\lambda_r$ .